

EXPERIMENTAL STUDY ON TURBULENT VELOCITY VECTOR FIELD OF HYDROGEN COMBUSTION BASED ON PARTICLE IMAGE VELOCIMETRY MEASUREMENT TECHNOLOGY

Bo Ran^{1,2}, Zhang Tianshuo^{1,2}, Song Zhangfeng^{1,2*}, Ma Hong^{1,2*}, Wu Jigang^{1,2}, Hao Kai^{1,2}

¹School of Mechanical Engineering, Hebei University of Architecture, Zhangjiakou, 075000, China

²Hebei Technology Innovation Center for Intelligent Production Line of Prefabricated Building Components, Zhangjiakou, 075000, China

Email*: szf2129@hebiace.edu.cn

Abstract - The investigation of turbulent flow fields reveals the evolutionary characteristics of multiscale turbulent flows, providing a core theoretical basis for combustion control, flow optimization, and stability analysis in engineering systems. Based on Particle Image Velocimetry technology, this study conducts experimental research on the multiscale nonlinear evolution of turbulent flow fields and their coupling mechanisms with energy transfer and mixing processes; to explore the spatiotemporal evolution of transient flow field properties under turbulent conditions, an experimental platform of a constant volume combustion bomb with controllable turbulent intensity and direction was established, where parameters of the turbulence generator and backpressure gradient ($P=1-5\text{bar}$) were systematically adjusted, and the Particle Image Velocimetry system was used to capture the motion of tracer particles with high precision instantaneous measurement. Experimental results indicate that the turbulent fluctuating velocity field exhibits a circular layered distribution characteristic with intensity increasing from the center to the periphery, and the velocity vector field is significantly enhanced as the intensity of turbulent disturbance increases; under the same disturbance intensity, an increase in backpressure gradient further intensifies the turbulence degree of the flow field; in addition, when the turbulent disturbance and backpressure reach a stable state, the influence of sampling time on the velocity vector field tends to stabilize. This study uncovers the interaction mechanism between pressure gradient and flow structure, the constructed experimental dataset provides a reliable benchmark calibration basis for turbulent numerical simulation in constant volume combustion bombs, and it also holds significant theoretical guiding value for the optimization of turbulence control strategies in related turbulent research.

Keywords: Particle Image Velocimetry measurement, Turbulence generator, Turbulent disturbance, Turbulent velocity vector field, Background pressure.

1. Introduction

With the continuous increasing in energy consumption and the growing severity of environmental pollution, improving the combustion efficiency of clean fuels and reducing pollutant emissions have become crucial research directions in the field of internal combustion engines (ICEs). In ICE power systems, the combustion of fuel primarily occurs in the form of turbulent premixed combustion. Therefore, a thorough investigation into the influence of turbulent flow on the combustion process holds significant guiding significance for revealing the intrinsic nature of turbulent

combustion and guiding the development of advanced combustion technologies [1-3].

Existing studies have demonstrated that the background pressure exerts a significant impact on turbulence intensity and scale. Currently, most research on turbulent flow focuses on the theoretical model simulation based on Computational Fluid Dynamics (CFD) technology, which has explored the distribution of turbulent flow fields under different background pressures [4-6]. However, the scarcity of experimental studies on the distribution of turbulent flow fields has restricted the validation and optimization of these models [7-12]. Consequently, based on a self-developed turbulent combustion

experimental platform with controllable intensity and direction, this study conducts experimental investigations on the effects of different turbulent disturbances, back pressures, and sampling times on the turbulent velocity vector field. The objective is to obtain experimental data that can support the validation and optimization of theoretical models. The conclusions derived from this research are of vital importance for detailed understanding and optimization of the turbulent flow process.

In this study, Particle Image Velocimetry (PIV) technology is employed. By measuring the instantaneous velocity of tracer particles in the turbulence generator under varying turbulent disturbances, back pressures, and sampling times, the velocity components of the tracer particles in two orthogonal directions within the turbulent velocity vector field are acquired [13, 14]. This work aims to provide a theoretical basis and fundamental experimental data support for further investigating the characteristics of the turbulent velocity vector field, analyzing the influence laws of different factors on the turbulent velocity vector field, and ultimately exploring the mechanism of turbulent combustion.

2. Turbulent Combustion Constant Volume Bomb Experimental Platform

The experiments were conducted on a self-developed experimental platform capable of controlling both the intensity and direction of turbulence. The platform comprises four main components: a turbulence generator, intake and exhaust systems, a Particle Image Velocimetry (PIV) measurement system, and a dynamic data acquisition system. The PIV system consists of a laser generator, a CCD camera, and a synchronization controller. The laser operates at a wavelength of 532 nm, with an adjustable repetition rate of 0–10 Hz, an energy output of 200 mJ, a pulse width of 6–9 ns, and a beam diameter of 9 mm. For velocity vector field measurements, a circular region with a diameter of 120 mm, centered on the chamber's midplane within the x–y measurement plane, was selected. A schematic diagram of the experimental principle is shown in Fig.1.

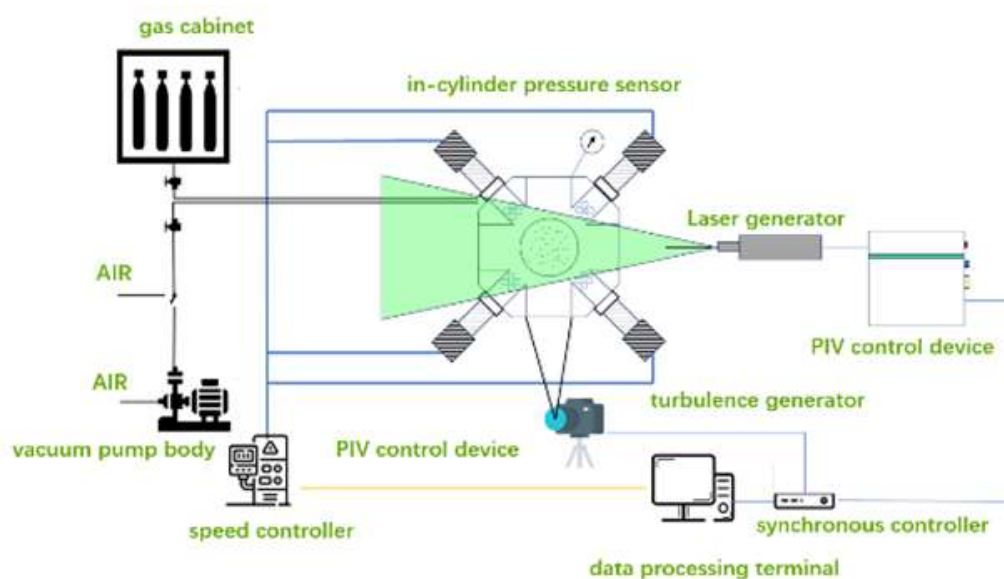


Figure 1: Schematic diagram of experimental principles

3. Results and Discussion

3.1. Principle of Velocity Vector Calculation in Particle Image Velocimetry

In PIV velocity vector calculations, interrogation areas are defined at the same spatial positions in two consecutive images captured at times t_0 and $t_0 + \Delta t$. The second image can be considered as a displaced version of the first image, corrupted by noise. The presence of noise significantly increases the computational complexity. However, for the system

noise considered here, the overall experimental error is approximately 0.2 pixels. During the experiments, the particle displacement between the two frames ranged from 6 to 10 pixels, resulting in a maximum measurement error of less than 4% [15, 16]. Therefore, noise effects were neglected in the present calculations.

$$g(m, n) \approx f(m, n) * s(m, n) \quad (1)$$

$$S(U, V) \approx \frac{F^*(U, V)G(U, V)}{|F(U, V)|} \quad (2)$$

$G(U,V)$, $F(U,V)$, and $S(U,V)$ denote the results of the discrete Fourier transform (DFT) of $f(m,n)$, $g(m,n)$, and $S(m,n)$, respectively; $F^*(U,V)$ represents the complex conjugate of $F(U,V)$. From Equation (2), $|F(U,V)|$ only modifies the magnitude of $S(U,V)$ without altering its position. It follows that:

$$\Phi(U,V) = F^*(U,V) G(U,V) \quad (3)$$

The inverse Fourier transform of $\phi(U,V)$ is computed, and the peak of $\phi(m,n)^2$ is detected to determine the particle displacement. From the detection results, it is found that the first image undergoes a displacement of D_x in the x-direction and D_y in the y-direction. The actual velocities V_x and V_y are obtained by multiplying the displacements by the scaling factor M and dividing by the time interval Δt .

$$V_x = \frac{D_x M}{\Delta t} \quad (4)$$

$$V_y = \frac{D_y M}{\Delta t} \quad (5)$$

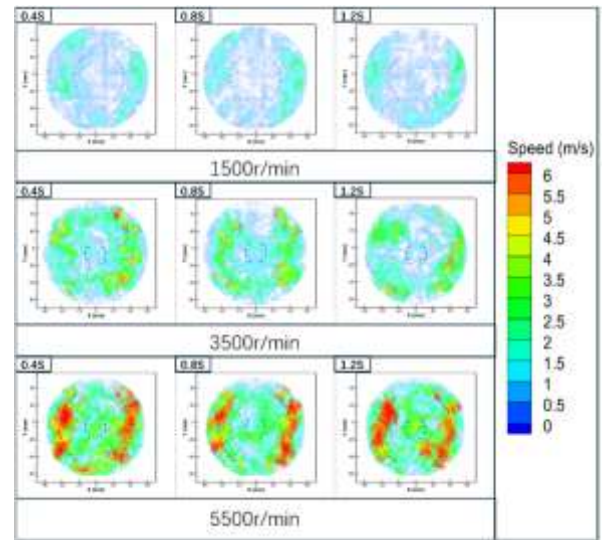
3.2. Effects of Turbulence Field Modifications on the Turbulent Velocity Vector Field

For visual clarity and ease of comparison, the same velocity color scale was used, enabling direct identification of the vector velocities based on color intensity. The velocity at each point represents the actual total velocity V_u , which is the vector sum of the measured velocity components V_x and V_y . The x- and y-coordinates correspond to the spatial positions within the measurement plane [17–19].

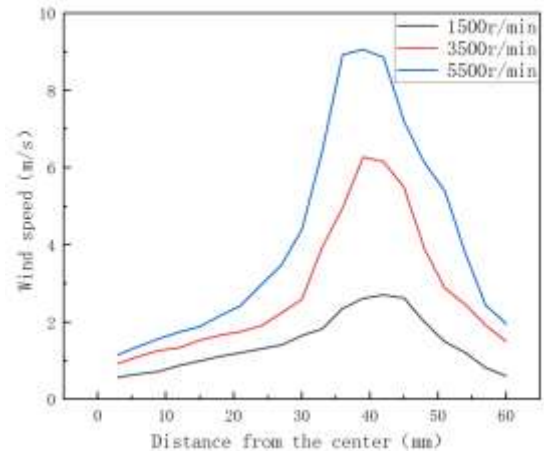
3.2.1. Turbulent Velocity Vector Fields in the Combustion Chamber under Different Turbulence Disturbance Intensities

Figure 2. presents the instantaneous velocity vector fields within the combustion chamber at different fan speeds of the turbulence generator, recorded under a constant background pressure of 3 bar. The tested fan speeds were 1500 rpm, 3500 rpm, and 5500 rpm. A direct comparison of the turbulent velocity vector maps reveals distinct differences between the low speed and high speed cases. Specifically, as the fan speed increases, the turbulent disturbance intensity rises significantly,

leading to a marked increase in the fluid velocity within the chamber. At the lower fan speed (1500 rpm), the turbulent velocity vector field exhibits a clear two layer structure, with minimal overall velocity variations across the field. In contrast, with increasing fan speed (3500 rpm and 5500 rpm), the velocity variations in the vector field become increasingly pronounced, and the layered structure is further enhanced.



(a) The turbulent velocity field measured by PIV



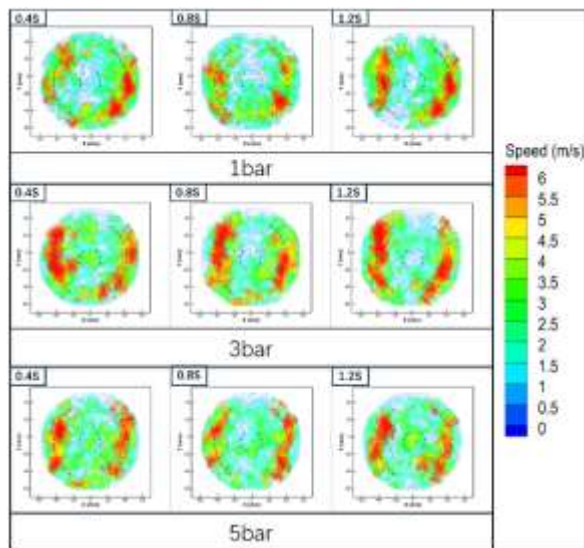
(b) Speed Comparison Graph

Figure 2: Turbulent Velocity Vector Field in the constant volume combustion bomb Under Different Rotational Speeds

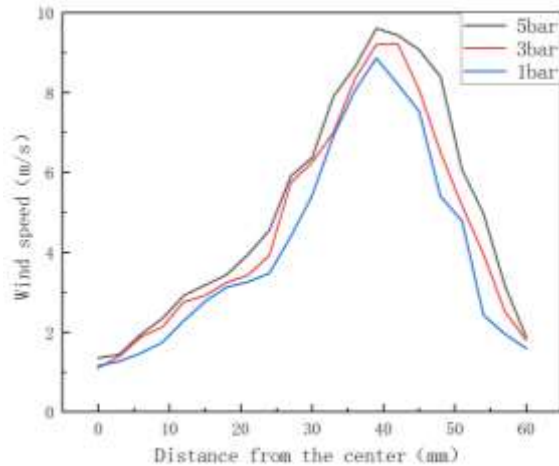
3.2.2. Effect of Back Pressure on the Turbulent Velocity Vector Field in the Combustion Chamber

Figure 3. presents the turbulent velocity vector fields within the combustion chamber at different back pressures. The experiments were conducted at a constant fan speed of 5500 rpm, with back pressures of 1 bar, 3 bar, and 5 bar; three instantaneous images were recorded for each pressure condition. Under identical turbulence

disturbance intensity, the influence of background pressure on the turbulent fluctuating velocity is observed to be relatively minor and is primarily confined to the central region of the chamber. Specifically, at lower back pressures, the area of low velocity flow at the center is more extensive, indicating weaker turbulence effects in this region. Conversely, increasing the background pressure under the same turbulence disturbance intensity results in an enhancement of the turbulent velocity at the central location.



(a) The turbulent velocity field measured by PIV



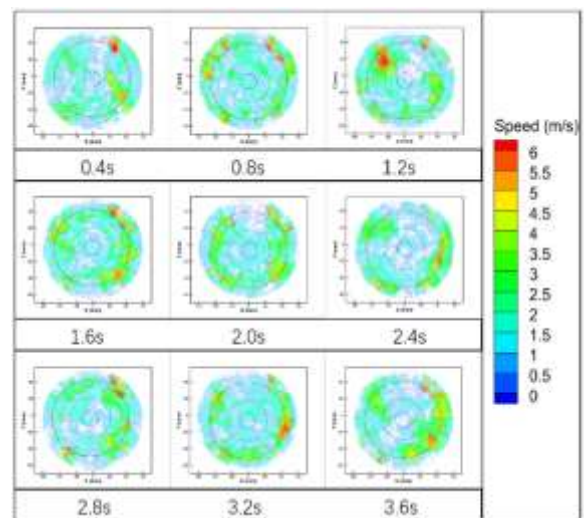
(b) Speed Comparison Graph

Figure 3: Turbulent Velocity Vector Field in a Constant Volume Combustion Bomb Under Different Pressures

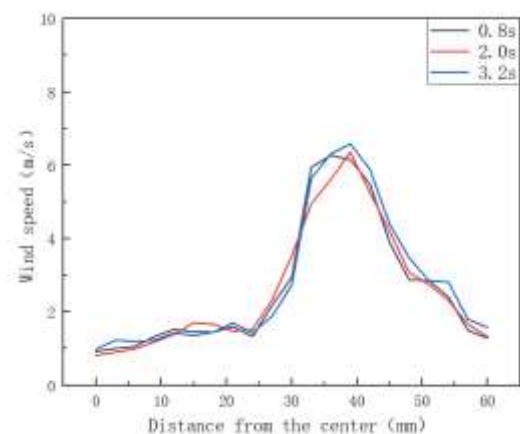
3.2.3 Turbulent Velocity Vector Fields in the Combustion Chamber at Different Time Instants

Fig.4. depicts the turbulent velocity vector fields within the combustion chamber at different sampling times, recorded under a constant background pressure of 3 bar and a turbulence generator fan speed of 3500 rpm. A total of nine

instantaneous images were captured at equal time intervals. Analysis of these results reveals that, with the turbulence disturbance intensity and back pressure held constant, variations in the sampling time do not produce significant differences in the turbulent velocity vector maps. The layered structure and turbulent velocities among the nine images are highly similar, indicating that the flow field remains in a relatively stable state. Under the premise of controlling other variables, changes in time have a negligible effect on the turbulent flow field, which maintains its stability over extended periods [20–22].



(a) The turbulent velocity field measured by PIV



(b) Speed Comparison Graph

Figure 4: Turbulent Velocity Vector Field in a Constant-Volume Combustion Bomb at Different Time Instants

4. Conclusions

In this study, an experimental investigation into the characteristics of the turbulent velocity vector field was conducted using a Particle Image Velocimetry (PIV) system combined with a self-developed experimental platform capable of controlling both

the intensity and direction of turbulence. Systematic experiments were performed to examine the variations in the turbulent velocity vector field under different conditions of turbulence disturbance, back pressure, and sampling time. Based on the experimental results, the x-y turbulent velocity vector field was established and analyzed, and the following conclusions are drawn.

The flow field exhibits an approximately circular layered distribution, where the turbulent vector velocity increases gradually from the center to the periphery. Notably, the fluid velocity is higher at the edge of the velocity vector map, i.e., in the region adjacent to the turbulence generator. This observation indicates that the turbulence generator in the present experimental platform is uniformly and reasonably arranged, and it generates an isotropic turbulent environment under a constant power input.

Inside the combustion chamber, the turbulent velocity vector field is most significantly influenced by the operating power of the turbulence generator. As the power increases, the turbulence disturbance intensity within the experimental platform rises sharply, leading to remarkably distinct changes in the turbulent velocity vector field. These results demonstrate that the variation of the turbulent flow field can be primarily regulated by controlling the turbulence disturbance.

With the turbulence generator power held constant (i.e., the turbulence disturbance intensity remaining essentially stable), analyses of the turbulent velocity vector maps obtained at different back pressures (ranging from 1 bar to 5 bar) reveal that both the flow velocity and turbulence intensity exhibit a slight increasing trend as the background pressure rises. However, this variation is not significant compared to the profound effects induced by increased turbulence disturbance intensity. Further analysis indicates that the influence of pressure on the turbulent velocity vector field is primarily concentrated in the central region of the flow field. At lower pressures, the low velocity zone in the central region of the combustion chamber is relatively extensive, resulting in suboptimal overall turbulence performance. As the pressure increases, the low velocity zone in the central region gradually shrinks, thereby optimizing the structure of the entire turbulent flow field.

With the turbulence generator power and back pressure maintained stable, the experimental results demonstrate that variations in sampling time do not induce substantial changes in the turbulent velocity vector field during the dynamic evolution of the turbulent flow field. In other words, when the

experimental platform operates in a steady state for prolonged experiments, the turbulent flow field remains stable, and no anomalies in the experimental results arise from fluctuations of the turbulent field.

Acknowledgement

This study was supported by the following projects: the Graduate Innovation Fund Project of Hebei University of Architecture and Civil Engineering (No. XY2024081); the Science and Technology Commissioner Project of Hebei Province (No. 2251639); the Science and Technology Fund Project of Hebei Provincial Department of Human Resources and Social Security: Research on the Impact of Digital Economy and Artificial Intelligence Development on the Employment Situation in Hebei Province and Its Countermeasures (No. JRS-2025-1041); The Sports Science and Technology Research Project of Hebei Province: Research on the High-Quality Development Strategy of the In-depth Integration of Ice and Snow Sports Culture and Tourism Public Resources in Hebei Province in the Post-Winter Olympics Era (No. 2026CY28).

References

- [1] Yao L. New energy utilization in environmental design and realization. *Energy Reports*, 2022, 8: 9211-9220.
- [2] Zhang F, Zhong S H. High-Fidelity Numerical Simulation of Turbulent Combustion Under Engine conditions. *Journal of Engineering Thermophysics*, 2024, 45(12): 3876-3898.
- [3] Qin S Y, Zhang X, Wang Y. A novel turbulent constant-volume combustion bomb flow field numerical analysis. *Journal of Automotive Engines*, 2019(6), 15-21.
- [4] Zhao F. Research on visual test technology of aeroengine temperature field based on laser diagnosis. *Laser Journal*, 46(1), 240-245.
- [5] Xu S J. Measurement Investigations of Turbulent Flow Field in a Constant Volume Combustion Chamber. *Huazhong University of Science and Technology*, 2017.
- [6] Xie Y, Sun Z Y. Effects of the external turbulence on centrally-ignited spherical unstable $\text{CH}_4/\text{H}_2/\text{air}$ flames in the constant-volume combustion bomb. *international journal of hydrogen energy*, 2019, 44(36): 20452-20461.
- [7] Zhao K, Lou D, Zhang Y, et al. Study on combustion and emission characteristics of hydrogen/air mixtures in a constant volume combustion bomb. *Renewable Energy*, 2024, 237: 121626.
- [8] Sun Z Y, Xu C S. Turbulent burning velocity of stoichiometric syngas flames with different hydrogen volumetric fractions upon constant-

- volume method with multi-zone model. *International Journal of Hydrogen Energy*, 2020, 45(7): 4969-4978.
- [9] Wang Y, Zhang X, Li Y. Numerical simulation of methane-hydrogen-air premixed combustion in turbulence. *International Journal of Hydrogen Energy*, 2023, 48(19): 7122-7133.
- [10] Li H, Li G, Zhang G. Self-similar propagation and flame acceleration of hydrogen-rich syngas turbulent expanding flames. *Fuel*, 2023, 350: 128813.
- [11] Xu S, Huang S, Huang R, et al. Estimation of turbulence characteristics from PIV in a high-pressure fan-stirred constant volume combustion chamber. *Applied Thermal Engineering*, 2017, 110: 346-355.
- [12] Wang Y, Zhang X, Li Y, et al. Experimental study on high pressure injection characteristics of gas fuel based on turbulent constant volume combustion bomb. *Energy Reports*, 2024, 11: 2306-2315.
- [13] Morsy M E. Studies of Laminar and Turbulent Combustion Using Particle Image Velocimetry, PhD thesis, p. 324, Uni. of Leeds, 2019.
- [14] Humphrey L J, Emerson B, Lieuwen T C. Premixed turbulent flame speed in an oscillating disturbance field. *Journal of Fluid Mechanics*, 2018, 835: 102-130.
- [15] McManus T A, Sutton J A. Simultaneous 2D filtered Rayleigh scattering thermometry and stereoscopic particle image velocimetry measurements in turbulent nonpremixed flames. *Experiments in Fluids*, 2020, 61: 1-19.
- [16] Wu Q, Zhu X Y, Xu C L. Research on high-resolution lightfield tomographic PIV technology based on physical equations. *Acta Optica Sinica*, 2025, 45(01): 146-157.
- [17] Zhang D, Zhou W, Huang H, et al. High-speed Gradient Flow Field Image Hybrid PIV-PSV Processing Algorithm. *Journal of Engineering Thermophysics*, 2024, 45(10): 3086-3090.
- [18] Wu P F, Liu B C, Lu Q L, et al. Experimental and numerical investigations on the interaction of flame and flowfield under combustion oscillation in the LPP combustor. *Journal of Engineering Thermophysics*, 2024, 45(6), 1579-1588.
- [19] Kondo C, Muramatsu K, Okamoto T. Effect of ambient pressure on fluorescence intensity of inexpensive inorganic fluorescent tracer for particle image velocimetry of gaseous flows near solid objects. *AIP Advances*, 2020, 10(3): 035010-035010-7.
- [20] Morsy M E, Yang J. Numerical and experimental study on turbulence statistics in a large fanstirred combustion vessel. *Experiments in Fluids*, 2021, 62(5): 116.
- [21] Bradley D, Lawes M, Morsy M E. Measurement of turbulence characteristics in a large scale fanstirred spherical vessel. *Journal of Turbulence*, 2019, 20(3): 195-213.
- [22] Manna O A, Mansour M S, Chung S H, et al. Characterization of turbulence in an optically accessible fanstirred spherical combustion chamber. *Combustion Science and Technology*, 2021, 193(7): 1231-1257